ARTICLES
PUBLISHED ONLINE: 22 NOVEMBER 2009 | DOI: 10.1038/NPHOTON.2009.218
nature photonics

Tuning a terahertz wire laser

Qi Qin[1], Benjamin S. Williams[1,2], Sushil Kumar[1], John L. Reno[3] and Qing Hu[1]*

Tunable terahertz lasers are desirable in applications in sensing and spectroscopy because many biochemical species have strong spectral fingerprints at terahertz frequencies. Conventionally, the frequency of a laser is tuned in a similar manner to a stringed musical instrument, in which pitch is varied by changing the length of the string (the longitudinal component of the wave vector) and/or its tension (the refractive index). However, such methods are difficult to implement in terahertz semiconductor lasers because of their poor outcoupling efficiencies. Here, we demonstrate a novel tuning mechanism based on a unique 'wire laser' device for which the transverse dimension w is $\ll\lambda$. Placing a movable object close to the wire laser manipulates a large fraction of the waveguided mode propagating outside the cavity, thereby tuning its resonant frequency. Continuous single-mode redshift and blueshift tuning is demonstrated for the same device by using either a dielectric or metallic movable object. In combination, this enables a frequency tuning of ~137 GHz (3.6%) from a single laser device at ~3.8 THz.

The terahertz frequency range (~1–10 THz or $\lambda \approx 30$–$300\ \mu$m) is rich with spectral fingerprints for sensing and imaging applications[1,2]. It is also among the most underdeveloped electromagnetic spectra[3,4]. This underdevelopment is largely due to the so-called 'terahertz gap' between solid-state electronic devices and photonic devices[5]. The recently developed terahertz quantum cascade lasers (QCLs) hold great promise as candidates to fill this technological gap[6]. The development of terahertz QCLs has been remarkable, particularly with regard to their output power levels and frequency coverage[7]. However, several major challenges remain. Among these is the lack of continuous tunability over a broad frequency range, which is necessary in sensing and spectroscopy applications.

Conventional laser tuning methods are difficult to implement at terahertz frequencies because of the relatively long wavelength λ compared to the cross-section w of semiconductor lasers. Continuous frequency tuning using an external-cavity grating has yet to be achieved[8], and electrical tuning by changing the refractive index due to temperature[9] or due to a cavity-pulling effect[10,11] produces a relatively small fractional tuning (<1%). Here, we demonstrate a novel tuning mechanism that qualitatively differs from all other methods[12]. This mechanism is based on the manipulation of the evanescent propagating mode of an unusual device termed a 'wire laser'[13], which is defined as a laser for which the dimension in the transverse direction w is much smaller than λ. To appreciate the difficulty in developing tunable terahertz QCLs and the novelty of the tuning mechanism in this work, it is instructive to analyse at a fundamental level how all lasers are tuned without introducing any intermediate variables such as effective mode index. In a uniform gain medium, the lasing frequency for a particular resonant mode is determined by its $\omega-k$ dispersion relation

$$k_z^2 + k_\perp^2 = \omega^2 \mu \varepsilon \qquad (1)$$

and the specific operation conditions. In equation (1), k_z and $k_\perp$ are the components of the **k**-vector in the longitudinal and transverse directions, respectively, ω is the frequency, $\mu \approx \mu_0$ is the permeability in vacuum and ε is the dielectric constant. The lasing frequency ω of an already fabricated device can be tuned by changing the values of k_z (Fig. 1a), $k_\perp$ (Fig. 1c) or ε (Fig. 1b). The dielectric constant ε can be tuned with temperature or electrically by carrier injection or a cavity-pulling effect. However, this tuning has a limited range (~30 GHz for suitably designed terahertz QCLs[9–11]). Most of the tunable lasers are tuned by changing k_z. Examples include changing the length of a Fabry–Pérot cavity formed with either a ridge[14] or a surface-emitting structure[15], changing the centre frequencies of distributed Bragg reflectors (DBR)[12], and changing the angle of an external-cavity grating[16]. Interestingly, these two mechanisms are the same as that used to tune a stringed musical instrument such as the violin, in which varying the length of a string corresponds to changing k_z, and varying the tension corresponds to changing ε. For sensing applications, mode-hop-free continuous tuning is required, which is usually achieved using an external-cavity grating. A broad range of tuning of ~24% has been demonstrated with mid-infrared QCLs[16]. At terahertz frequencies, because of the long wavelengths ($\lambda \approx 100\ \mu$m) compared to the subwavelength dimension w of the laser facet, it is difficult to focus a large fraction of the beam diffracted from the grating back to the gain medium. This difficulty is further exacerbated by the cryogenic conditions that are necessary for operation. As a result, continuous tuning based on this well-developed technique has not been achieved at terahertz frequencies[8]. In contrast, instead of fighting the battle with brute force, the new tuning mechanism demonstrated here actually takes advantage of the small cross-section relative to the wavelength, and is achieved in the extreme limit $w/\lambda \ll 1$.

Of the three parameters that determine the lasing frequency (k_z, $k_\perp$ and ε), very little effort has been made to change $k_\perp$ (ref. 17). This is because in most solid-state and semiconductor lasers, λ is comparable with, or often smaller than, the transverse dimension of the cavity w. Consequently, little mode leaks out in the transverse directions and very little change can be made to $k_\perp$. For terahertz QCLs based on metal–metal waveguides[18–20], laser ridges can be made with deep subwavelength size in the transverse dimensions. Such lasers showed unexpected radiation patterns with strong interference structures[21]. In a subsequent paper analysing the radiation patterns using an antenna model, such interference patterns are attributed to the mode attached to a 'wire laser', which is defined

[1]Department of Electrical Engineering and Computer Science and Research Laboratory of Electronics, Massachusetts Institute of Technology, Cambridge, Massachusetts 02139, USA, [2]Department of Electrical Engineering and California NanoSystems Institute, University of California, Los Angeles, California 90095, USA, [3]Sandia National Laboratories, Department 1123, MS 0601, Albuquerque, New Mexico 87185-0601, USA. *e-mail: qhu@mit.edu

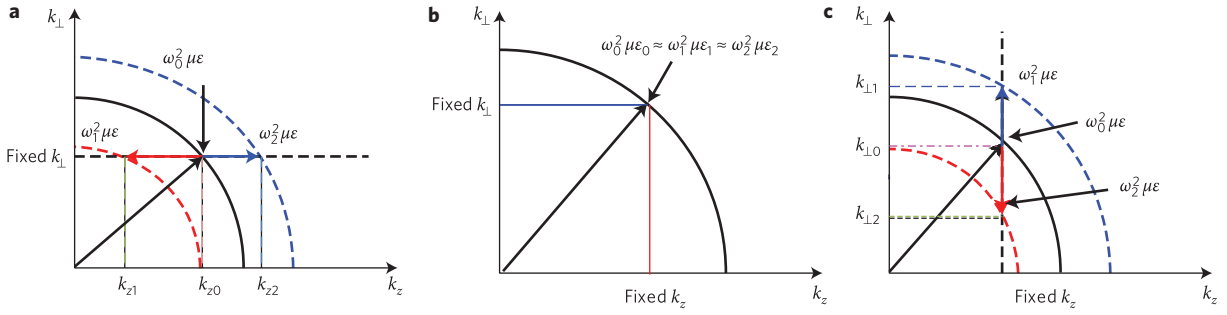

Figure 1 | Illustration of different tuning mechanisms. The curves relating the transverse wave vector ($k_\perp$) and longitudinal wave vector (k_z) are based on equation (1), which is the dispersion relation in a uniform gain medium. The lasing frequency ω is determined by the radius of a particular curve that intersects a specific value of $k_\perp$ and k_z, which are determined by operating conditions. The black curves represent the condition that determines the original frequency ω_0 of a laser without tuning. The blue and red dashed curves represent the conditions for which the laser tuning is either blue- or redshifted. **a**, The most commonly used tuning mechanism, in which both ε and $k_\perp$ are fixed and the lasing frequency is tuned by changing k_z. This can be accomplished by changing the cavity length of a Fabry–Pérot laser, or changing the centre wavelength of distributed Bragg reflectors (DBRs), or changing the angle of an external-cavity grating. **b**, Arrangement with both $k_\perp$ and k_z fixed. The tuning is achieved by changing the dielectric constant ε, which can be accomplished with temperature tuning or electrical bias. **c**, The tuning scheme of the present work, in which the frequency of a wire laser is tuned by directly changing the transverse wave vector $k_\perp$.

as a laser with a deep subwavelength cross-section such that a substantial fraction of the mode travels outside the solid core[13]. This unusual feature allows tuning of the lasing frequency by changing $k_\perp$, as demonstrated in the present work. Such a tuning mechanism has no analogue with the aforementioned example of a stringed musical instrument, because changing the diameter of a string also modifies the sound velocity, in a similar manner to changing the refractive index in a laser. It should be clarified that the term 'wire laser' in this letter refers to w relative to the wavelength λ rather than the absolute size, with the implication $w/\lambda \ll 1$. The similar term 'nanowire laser' is typically used for lasers with a transverse dimension on the scale of nanometres, but they function with a relative dimension $w/\lambda \approx 1$ or greater[22–24].

Figure 2 describes the concept of tuning in a visual form. A movable object, called a 'plunger' hereinafter, is placed along the side of a terahertz wire laser. The gap between the plunger and the laser can be adjusted mechanically. In this work, which aims to demonstrate the principle of operation, the plunger can only be pushed towards the laser, irreversibly. Figure 2a,b illustrates tuning both to a lower frequency (redshift) and a higher frequency (blueshift) with this mechanism. If a dielectric plunger is used (silicon in this work), as it is pushed towards the laser, it extracts the mode from the gain medium, effectively expanding the mode profile in the transverse direction, as shown in Fig. 2a. Consequently, the value of $k_\perp$ decreases, and from equation (1) and Fig. 1c, a redshift tuning is achieved. Similarly, if a metal plunger is used (gold in this work), $k_\perp$ increases as the plunger is pushed towards the laser as the mode approaches cutoff in the transverse dimension, resulting in a blueshift tuning. In the context of dielectric waveguides, such a situation should result in a greater 'effective mode index' n_{eff} as the mode is pushed into the solid core and a larger mode fraction occupies the region where $\varepsilon > \varepsilon_0$, resulting in a greater mode confinement factor. However, writing $k_z = n_{\mathrm{eff}}(\omega/c)$ suggests that the parameter n_{eff} actually decreases due to the blueshift in ω (note that k_z is kept fixed by the grating periodicity), which is counterintuitive to conventional understanding. Hence, to avoid confusion, this tuning mechanism is best described by considering the variation of the parameter $k_\perp$ instead of the parameter n_{eff}.

The actual experimental implementation of the setup is shown in Fig. 3a–d. Figure 3f shows the calculated laser frequency as a function of the gap between the plunger and the laser ridge (for a parallel configuration). Combining blue- and redshift tuning, a total tuning range of ~430 GHz can be achieved if the plunger can be brought to within ~0.5 μm of the laser, for which the average width of ~12 μm is much smaller than the wavelength (~80 μm) at ~3.8 THz. This broad tuning range is still within the gain bandwidth of the resonant-phonon gain medium, which has shown simultaneous lasing over a frequency range of ~550 GHz (refs 9,25). To ensure continuous tuning of a single lasing mode, first-order distributed feedback (DFB) gratings were designed and fabricated[25], as shown in Figs 2 and 3. For this particular purpose, an asymmetric DFB corrugation structure was used, with the flat side facing the plunger. The DFB corrugation was placed on the opposite side. We chose a sinusoidal modulation in the DFB for a smooth side wall. The laser ridge had an average width of 12.5 μm, sinusoidal grating modulation of 3 μm, 30 periods and a grating period of $\Lambda = 13.7$ μm. The design of the DFB/plunger structure was aided with finite-element (FEM) simulations using a commercial software package (Comsol 3.2). The metal was treated as a perfect conductor and the semiconductor was undoped. So the calculated gain threshold g_{th} only reflected radiative losses. For a bare DFB laser, writing $k_z = n_{\mathrm{eff}}(\omega/c) = \pi/\Lambda$, an effective mode index of $n_{\mathrm{eff}} \approx 2.86$ was estimated for the lowest loss mode, which is considerably lower than the refractive index of the active medium ($n_{\mathrm{active}} = 3.6$ used for calculation[9]) and is indicative of a large fraction of the mode propagating outside the active medium.

In the longitudinal direction under the resonance condition $k_z = \pi/\Lambda$, where Λ is the grating period, two standing-wave solutions exist and each at a different frequency, forming a bandgap. The upper band-edge mode has the maximum intensity localized at the narrow part of the grating, which results in a larger value of $k_\perp$. Similarly, the maximum intensity of the lower band-edge mode is located at the wider part of the grating. Meanwhile, the front facet, from which the radiation is coupled out, is open and can be defined by dry etching. By carefully designing the position of the front facet relative to the DFB grating, either the lower band-edge or the upper band-edge mode will have lower radiation loss, and will be the lasing mode in a single-mode operation. To enhance the tuning range, the upper band-edge mode was chosen to be the lasing mode. This can be understood by envisioning that as a metal plunger is pushed towards the laser, it pushes the mode towards the DFB corrugation, increasing its coupling with the grating and therefore the bandgap (from ~260 to ~417 GHz with a gap of 0.5 μm). This increase of the bandgap will accentuate the blueshift tuning discussed earlier. Similarly, as a silicon plunger is pushed towards the laser, it extracts the mode away from the DFB corrugation and shrinks the bandgap (from ~260 to ~120 GHz with a gap of 0.5 μm), effectively enhancing the redshift tuning.

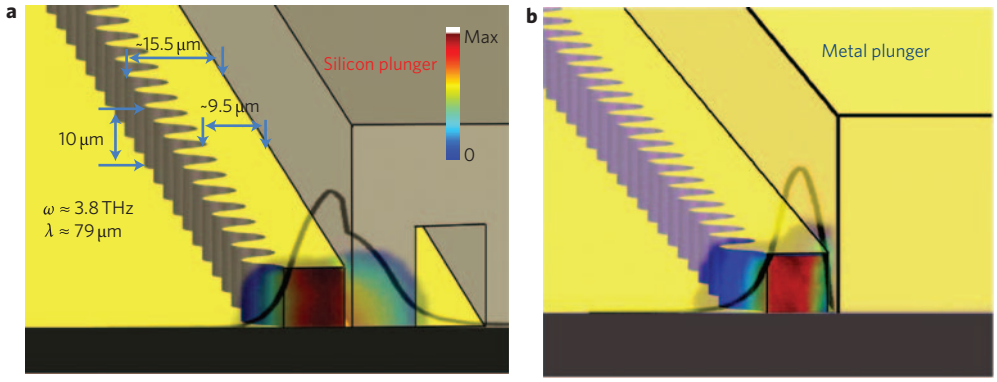

Figure 2 | The concept of tuning a wire laser. A wire laser is a unique device that has deep subwavelength transverse dimensions[13], and consequently a large fraction of the electromagnetic mode resides outside the gain medium. In this work, it is a metal–metal ridge waveguide with sinusoidal corrugations on one side that provide first-order distributed feedback to achieve single-mode operation[25]. The transverse mode outside the solid core can be manipulated by a movable object to change the resonant frequency of the cavity to tune the laser. **a**,**b**, Schematics illustrating the tuning mechanism with a silicon plunger (**a**) and a metallic plunger (**b**). The gap between the sidewall of the laser and the plunger is ~1 μm. The electrical field profile at the laser facet is shown at the narrowest cross-section of the DFB structure. The dark curve is the mode profile obtained by integrating the electrical field component perpendicular to the ground plane. By squeezing or extending the mode in the transverse dimension, the metal or silicon plunger can tune the frequency to the blue or red side of a stand-alone cavity without the plunger. A cave in the silicon plunger defines the width of this plunger to be ~13 μm. This relatively small width (required only for the silicon plunger) is essential to assure a sufficient mode overlap with the gain medium to achieve lasing.

Based on this design consideration, the front facet was chosen to be at the widest part of the DFB grating (Fig. 3d), which increases the radiation loss of the lower band-edge mode and its lasing threshold. The lasing frequency (the upper band-edge mode) of an isolated DFB laser is designed to be ~3.8 THz, which is close to the centre frequency of the gain medium (labelled FL183S, growth VA0094, a resonant-phonon design similar to that in ref. 26) measured from Fabry–Pérot ridge devices. It is clear in this configuration, where $k_z = \pi/\Lambda$ is fixed during operation, that tuning can only be achieved by changing $k_\perp$ (Fig. 1c). Finally, the rear facet of the laser is defined, using wet etching, with a slope, so that a bonding pad can be fabricated away from the laser and the electrical contact to the top metal plate can be made without interfering with the movement of the plunger (Fig. 3c).

The height of the terahertz gain medium was ~10 μm. In the same fabrication process that defined the DFB laser ridges, rails perpendicular to the laser ridges to guide the plungers were also fabricated, as illustrated in Fig. 3c. The length of these guide rails was also precisely defined to prevent the plunger from 'plunging' into the DFB ridges. Because of this consideration, the side wall of the plunger facing the laser ridge was defined using dry etching, along with slots matching the guiding rails with stoppers at the other end of the guide rail (not shown in the figure). As a result, the actual plunger used in the experiment had an overhang over the laser ridge, as shown in Fig. 3d. Our simulation shows that this overhang has little effect on the tuning process because it is ~7 μm higher than the top of the laser, where the evanescent mode is negligible. For a silicon plunger, a reduced width is also required so that the mode remains appreciably in the gain medium to achieve lasing. This reduced width is also defined using dry etching and is shown in Fig. 3d. During operations, the plunger is pressed down and can only be pushed forward towards the laser ridge. The whole block is mounted on a cold plate in a vacuum cryostat during testing. The emitted laser light is collected without any optical components inside the cryostat. All the spectra were measured at 5 K using a Nicolet 850 spectrometer (purged with N_2 gas) and a germanium: gallium photodetector in pulse mode with a frequency of 90 kHz and a duration of 200 ns.

A great challenge in this proof-of-concept demonstration was to overcome the friction between the plunger and the guiding rails. A piezoelectric-transducer (PZT) bender (P-871.140 Piezo Bender Actuator, http://www.physikinstrumente.com/en/products/prspecs.php?sortnr=101780) was initially used. This bender has a continuous displacement range of 800 μm in either direction at room temperature, although data for cryogenic temperatures are not available. However, with this set-up, continuous tuning was difficult to achieve. This problem was identified as a known stick–slip effect[27,28] resulting from the difference between the static and dynamic friction when the plunger moves on the rails, which often causes an abrupt and discontinuous movement of the plunger. To overcome this problem, a mechanical differential micrometer was used, which had a movement resolution of 0.5 μm. This resolution was further improved by using a ~4:1 lever, as shown in Fig. 3a, resulting in a ~140-nm step resolution. This mechanical module was mostly made of steel with the exception of the thermal isolator, which was composed of fibre glass. This was therefore much stiffer than the PZT bender, allowing a greater pushing force to overcome the large static friction, resulting in a less abrupt movement of the plunger.

Tuning was achieved by using both the differential micrometer and the PZT bender. The results with the broadest tuning range, including both redshift and blueshift, from a single device are shown in Fig. 4. With plungers, a redshift tuning of 57 GHz and a blueshift of 80 GHz were achieved. In combination, a total tuning of 137 GHz, or ~3.6% fractional tuning, was achieved. During the spectral measurements, both the device bias and the temperature were kept constant, so tuning due to Stark shift and/or temperature was negligible. In fact, the frequency shift of the DFB device with bias, with the plunger in a fixed position, was not measurable within the resolution (3.75 GHz) of the spectrometer. Hence, the frequency shift of the single lasing mode, shown in Fig. 4, can be unambiguously attributed to the tuning of $k_\perp$ by the movement of the plunger. The redshift tuning with the silicon plunger and blueshift tuning with the metal plunger are also consistent with our predictions. Together, these results have firmly established the novel tuning mechanism discussed in this Letter.

The total tuning range of ~137 GHz, although impressive and far greater than results achieved with terahertz QCLs, is far less than the calculated result of ~430 GHz shown in Fig. 3f. This discrepancy can be explained with several possible scenarios. First, the calculation in Fig. 3f assumes a perfect parallel alignment between the plunger and the flat side of the DFB laser ridge. If

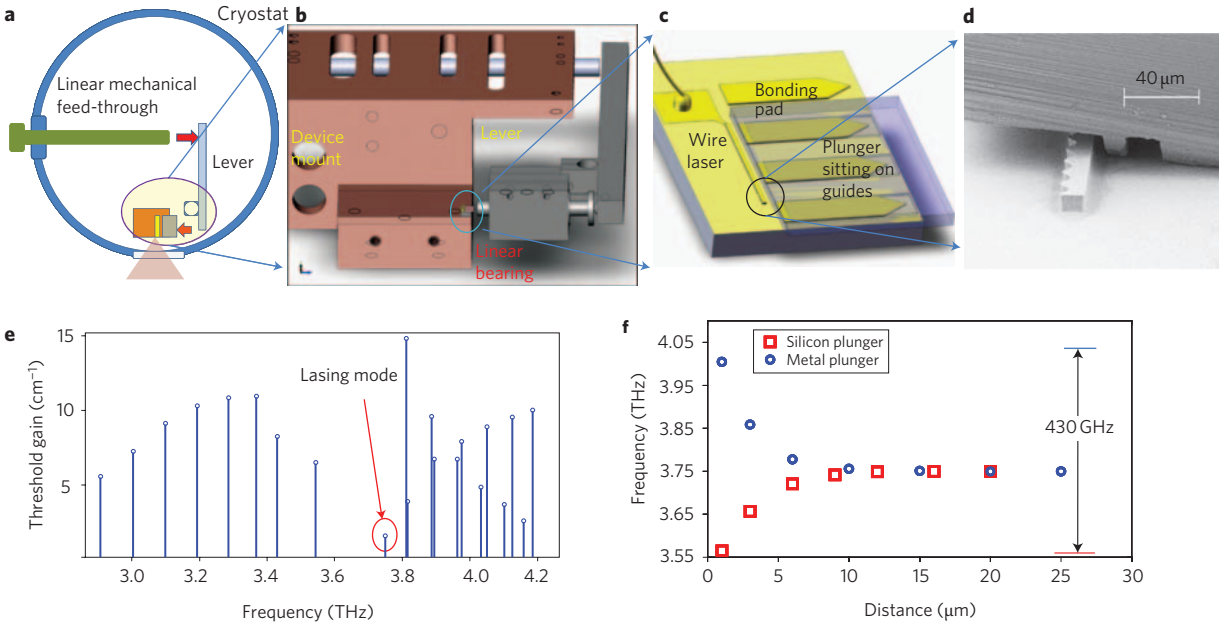

Figure 3 | Experimental setup and simulation results. a, Schematic of the experimental setup, in which a differential micrometer is used to push the long end of a lever, the short end of which in turn pushes a plunger. **b**, Three-dimensional structure of device mount (copper colour) and mechanical module (silver colour), showing the device is mounted in the lower-right corner. **c**, Enlarged view of the device region in **b**, showing the plunger (transparent blue) lying on top of guide rails, ready to be actuated by the shaft of a linear bearing. The yellow colour represents metallic parts. The overhang of the plunger on the laser ridge (as seen in **d**) is omitted for clarity. **d**, Scanning electron microscopy image of an assembled device with a silicon plunger. To show the configuration clearly, the silicon plunger is shorter than the ridge so the front facet of the laser can be seen. In actual measurements, the plunger covers the entire laser ridge. **e**, Grating mode spectra of a DFB device. The radiation loss from the open facet is plotted. This open facet is chosen at the widest location to select the fundamental upper band-edge mode as the lasing mode, as highlighted by the red circle. **f**, Calculated lasing frequency as a function of the distance of the plunger to the device.

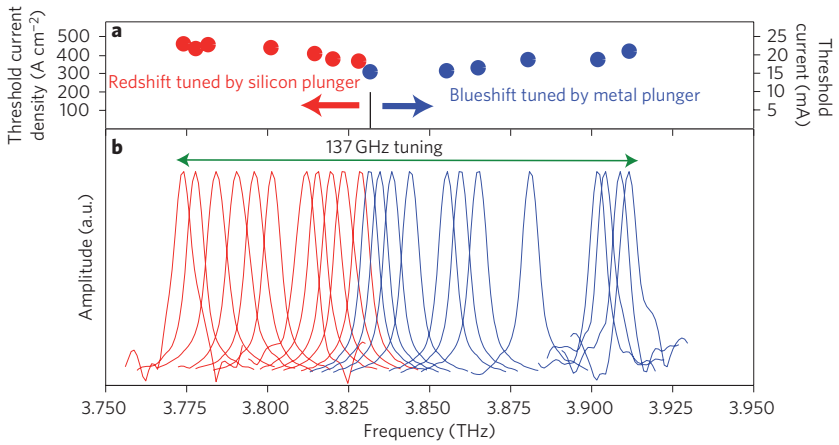

Figure 4 | Tuning results from device T114. The device has an average width of 12.5 μm, a sinusoidal grating amplitude of 3 μm, periodicity of 13.7 μm and 30 periods. The blue and red colours indicate the blueshift of frequency as tuned by a gold plunger and redshift by a silicon plunger. When operated without the plunger assembly, the device lased at the same frequency (~3.83 THz) as it did when the plunger was placed far away (25 μm in this case). **a**, Threshold current densities of the device at different frequencies, showing a moderate increase as the plunger is pushed towards the laser ridge. **b**, Broadband tuning of the device over a range of 137 GHz. All the spectra were recorded under the same drive current and temperature conditions. The small discontinuity is due to the stick-slip effect.

the alignment is slightly off, even by 1°, the tuning range will be reduced by more than a factor of two. Such a misalignment can certainly not be ruled out in this proof-of-concept demonstration. Second, as can be seen from Fig. 3f, most of the tuning is achieved with the plunger very close (<5 μm) to the laser ridge. Controlled movement of the plunger in such a close range is difficult to achieve with the present setup.

The measured power levels change with the plunger position in a complicated way, due to the changes in beam pattern and in atmospheric attenuation with frequency. Also, the absolute power was too low in this experiment to be measurable with a power meter because the assembly required the device to be placed far from the Dewar window and did not allow the use of a collecting optic such as a metallic cone to collect the highly divergent beam[21] emitted from the

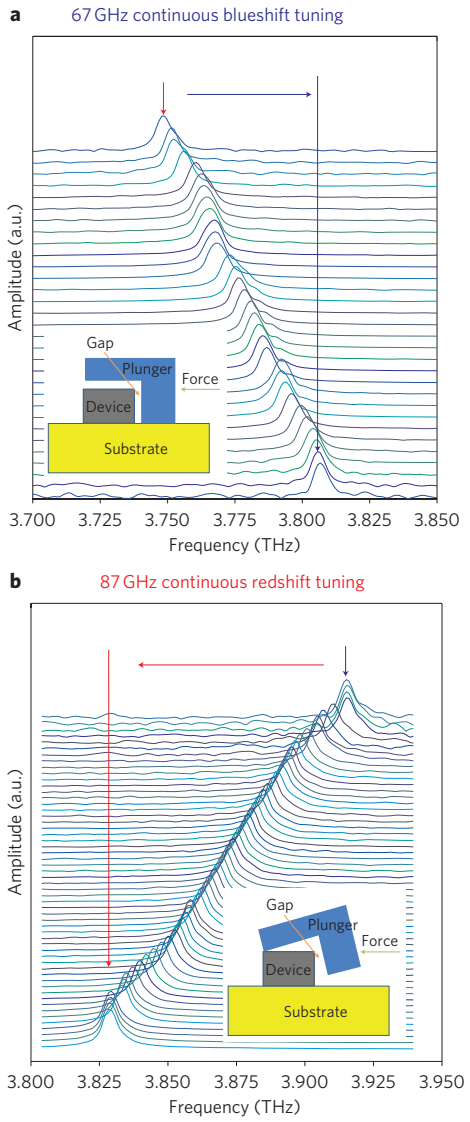

Figure 5 | Continuous tuning spectra. a, Continuous tuning of a device with a gold plunger over a range of 67 GHz. The device has an average width of 14.5 μm, sinusoidal grating amplitude of 3 μm, periodicity of 17.1 μm and 30 periods. All the spectra were recorded under the same drive current and temperature conditions. **b**, Abnormal but continuous redshift tuning result for device T13, with a gold plunger, over a range of 87 GHz. The device has an average width of 12.5 μm, sinusoidal grating amplitude of 3 μm, periodicity of 13.7 μm and 30 periods. The tuning was redshifted when the plunger was pushed due to the roll-over movement, and is reversible for this particular case. The increased gap between the plunger and device during this process causes the abnormal redshift, as illustrated in the inset.

laser facet. Thus, a more meaningful parameter for characterizing the laser performance is the threshold current at different plunger positions. This result is shown in the upper panel in Fig. 4, which exhibits a moderate increase as either a silicon or a metal plunger is pushed towards the laser ridge. For the silicon plunger, this increase is due to a reduction of the mode confinement factor in the gain medium. For the metal plunger, the increase of the lasing threshold is likely due to the loss of the metal and a thin SiN insulation layer preventing shorting the plunger with the device.

The tuning spectra in Fig. 4 show some discontinuous jumps, likely due to the stick–slip effect mentioned earlier. Because of this effect, measurement was not consistent between runs. Figure 5 shows clearer evidence of continuous tuning, although with smaller tuning ranges, from two measurements on different DFB devices. Figure 5a shows a continuous blueshift tuning using a metal plunger, as expected. The result from Fig. 5b is also from a metal plunger. However, it shows a redshift tuning. This puzzling result was resolved when the set-up was inspected under a microscope at room temperature. It became clear that the plunger had been tilted inadvertently, and its overhang was hinged on the edge of the laser ridge, as illustrated in the inset in Fig. 5b. As the upper part of the metal plunger is pushed forward, the plunger is further tilted and the effective gap between the plunger and the laser ridge increases, resulting in the observed redshift tuning. Interestingly, free from the friction problem, this scheme allows a reversible tuning, as a retreat of the bender relaxes the tilt of the plunger, yielding a blueshift.

The novel tuning mechanism of laser frequency, demonstrated here by changing $k_{\perp}$, applies to wire lasers at any frequencies. For recently developed wire lasers at visible frequencies[29], one could envision using a scanning probe to manipulate the transverse mode profile to tune the frequency for sensing and spectroscopy at nanometre scales. For terahertz wire lasers, further development based on MEMS (micro-electro-mechanical systems) technology will allow a better control of the plunger, which will result in a finer tuning over a broader frequency range in a reversible way. Such a controlled tuning will also offer a mechanism for frequency stabilization using feedback control. Finally, the generated tunable single-mode signal from a wire laser can be fed into an integrated terahertz amplifier to produce high-power radiation with good beam patterns[30].

Received 1 June 2009; accepted 26 October 2009;
published online 22 November 2009

References

1. Mittleman, D. (ed.) *Sensing with Terahertz Radiation* (Springer, 2003).
2. Davies, A. G., Linfield, E. H. & Pepper, M. The terahertz gap: the generation of far-infrared radiation and its applications. *Phil. Trans. R. Soc. Lond. A* **362,** 195–414 (2004).
3. Siegel, P. H. Terahertz technology. *IEEE Trans. Microwave Theory Tech.* **50,** 910–928 (2002).
4. Tonouchi, M. Cutting-edge terahertz technology. *Nature Photon.* **1,** 97–105 (2007).
5. Lee, M. & Wanke, M. C. Searching for a solid-state terahertz technology. *Science* **316,** 64–65 (2007).
6. Köhler, R. *et al.* Terahertz semiconductor–heterostructure laser. *Nature* **417,** 156–159 (2002).
7. Williams, B. S. Terahertz quantum-cascade lasers. *Nature Photon.* **1,** 517–525 (2007).
8. Lee, A. W. M., Qin, Q., Kumar, S., Hu, Q. & Reno, J. L. Frequency-tunable external cavity terahertz quantum cascade laser. In *Conference on Lasers and Electro-Optics/International Quantum Electronics Conference. OSA Technical Digest (CD)*, paper CThH5 (Optical Society of America, 2009).
9. Kumar, S. *et al.* Surface-emitting distributed feedback terahertz quantum-cascade lasers in metal–metal waveguides. *Opt. Express* **15,** 113–128 (2007).
10. Dunbar, L. A. *et al.* Small optical volume terahertz emitting microdisk quantum cascade lasers. *Appl. Phys. Lett.* **90,** 141114 (2007).
11. Zhang, H. *et al.* Terahertz photonic crystal quantum cascade lasers. *Opt. Express* **15,** 16818–16827 (2007).
12. Buus, J., Amann, M.-C. & Blumenthal, D. J. *Tunable Laser Diodes and Related Optical Sources* (John Wiley & Sons, 2005).
13. Orlova, E. E. *et al.* Antenna model for wire lasers. *Phys. Rev. Lett.* **96,** 173904 (2006).
14. Xu, J. *et al.* Tunable THz quantum cascade lasers with an external cavity. *Appl. Phys. Lett.* **91,** 121104 (2007).
15. Huang, M. C. Y., Zhou, Y. & Chang-Hasnain, C. J. A nanoelectromechanical tunable laser. *Nature Photon.* **2,** 180–184 (2008).
16. Maulini, R. *et al.* External cavity quantum-cascade laser tunable from 8.2 to 10.4 μm using a gain element with a heterogeneous cascade. *Appl. Phys. Lett.* **88,** 201113 (2006).
17. Amann, M.-C., Illek, S., Schanen, C. & Thulke, W. Tunable twin-guide laser: a novel laser diode with improved tuning performance. *Appl. Phys. Lett.* **54,** 2532–2533 (1989).
18. Williams, B. S., Kumar, S., Callebaut, H., Hu, Q. & Reno, J. L. Terahertz quantum-cascade laser at $\lambda \approx 100$ μm using metal waveguide for mode confinement. *Appl. Phys. Lett.* **83,** 2124–2126 (2003).

19. Kohen, S., Williams, B. S. & Hu, Q. Electromagnetic modeling of terahertz quantum cascade laser waveguides and resonators. *J. Appl. Phys.* **97,** 053106 (2005).
20. Hu, Q. *et al.* Resonant-phonon-assisted THz quantum-cascade lasers with metal–metal waveguides. *Semicond. Sci. Technol.* **20,** S228–S236 (2005).
21. Adam, A. J. L. *et al.* Beam patterns of terahertz quantum cascade lasers with subwavelength cavity dimensions. *Appl. Phys. Lett.* **88,** 151105 (2006).
22. Huang, M. H. *et al.* Room-temperature ultraviolet nanowire nanolasers. *Science* **292,** 1897–1899 (2001).
23. Duan, X. *et al.* Single-nanowire electrically driven lasers. *Nature* **421,** 241–245 (2003).
24. Zimmler, M. A. *et al.* Laser action in nanowires: observation of the transition from amplified spontaneous emission to laser oscillation. *Appl. Phys. Lett.* **93,** 051101 (2008).
25. Williams, B. S., Kumar, S., Hu, Q. & Reno, J. L. Distributed-feedback terahertz quantum-cascade lasers with laterally corrugated metal waveguides. *Opt. Lett.* **30,** 2909–2911 (2005).
26. Williams, B. S., Kumar, S., Hu, Q. & Reno, J. L. Operation of terahertz quantum-cascade lasers at 164 K in pulsed mode and at 117 K in continuous-wave mode. *Opt. Express* **13,** 3331–3339 (2005).
27. Baumberger, T., Heslot, F. & Perrin, B. Crossover from creep to inertial motion in friction dynamics. *Nature* **367,** 544–546 (1994).
28. Braun, O. M. & Naumovets, A. G. Nanotribology: microscopic mechanisms of friction. *Surf. Sci. Rep.* **60,** 79–158 (2006).
29. Rupert, F. O. *et al.* Plasmon lasers at deep subwavelength scale. *Nature* **461,** 629–632 (2009).
30. Mauro, C. *et al.* Amplification of terahertz radiation in quantum cascade structures. *J. Appl. Phys.* **102,** 063101 (2007).

Acknowledgements

This work was supported by the Air Force Office of Scientific Research, National Aeronautics and Space Administration, and National Science Foundation. Sandia is a multiprogram laboratory operated by Sandia Corporation, a Lockheed Martin Company, for the United States Department of Energy under contract no. DE-AC04-94AL85000.

Additional information

Reprints and permission information is available online at http://npg.nature.com/reprintsandpermissions/. Correspondence and requests for materials should be addressed to Q.H.